Available online at www.sciencedirect.com
ScienceDirect
Journal of Power Sources 179 (2008) 576–583
JOURNAL OF POWER SOURCES
www.elsevier.com/locate/jpowsour

A modified suspension spray combined with particle gradation method for preparation of protonic ceramic membrane fuel cells

Kui Xie [a], Ruiqiang Yan [b], Dehua Dong [c], Songlin Wang [a], Xiaorui Chen [a], Tao Jiang [a], Bin Lin [a], Ming Wei [a], Xingqin Liu [a,*], Guangyao Meng [a]

[a] *Department of Materials Science and Engineering, University of Science and Technology of China, Hefei, Anhui 230026, China*
[b] *Department of Materials Engineering, Taizhou University, Linhai, Zhejiang 317000, China*
[c] *Department of Chemical Engineering, Monash University, Clayton, VIC 3800, Australia*

Received 16 January 2008; received in revised form 29 January 2008; accepted 29 January 2008
Available online 7 February 2008

Abstract

In order to prepare a dense proton-conductive $Ba(Zr_{0.1}Ce_{0.7})Y_{0.2}O_{3-\delta}$ (BZCY7) electrolyte membrane, a proper anode composition with 65% Ni_2O_3 in weight ratio was determined after investigating the effects of anode compositions on anode shrinkages for co-sintering. The thermal expansion margins between sintered anodes and electrolytes, which were less than 1% below 750 °C, also showed good thermal expansion compatibility. A suspension spray combined with particle gradation method had been introduced to prepare dense electrolyte membrane on porous anode support. After a heat treatment at 1400 °C for 5 h, a cell with $La_{0.5}Sr_{0.5}CoO_{3-\delta}$ (LSCO) cathode was assembled and tested with hydrogen and ammonia as fuels. The outputs reached as high as 330 mW cm^{-2} in hydrogen and 300 mW cm^{-2} in ammonia at 700 °C, respectively. Comparing with the interface of another cell prepared by dry-pressing method, this one also showed a good interface contact between electrodes and electrolyte. To sum up, this combined technique can be considered as commercial fabrication technology candidate.

Keywords: Solid oxide fuel cells; $BaZr_{0.1}Ce_{0.7}Y_{0.2}O_{3-\delta}$; Suspension spray; Interface; Particle gradation

1. Introduction

Solid oxide fuel cells (SOFCs) now develop into their new stage characterized with thin electrolyte membranes on porous electrode supports [1]. The most important fabrication techniques developed for SOFCs are almost all concerned with inorganic electrolyte membranes. Therefore, SOFCs can also be named as ceramic membrane fuel cells (CMFCs). CMFCs based on proton electrolytes (CMFC-H) may exhibit more advantages than the ones based on oxygen-ion electrolytes (CMFC-O) in many respects, such as low activation energy [1] and high energy efficiency [2]. Many perovskite-type oxides, used as protonic electrolyte for CMFCs, show high proton conductivity in a reducing atmosphere [3–8]. These proton conductors in wet atmosphere will produce proton defect as charge carrier, which can be written as following [4]:

$$H_2O + V_O^{\bullet\bullet} + O_O^{x} \Leftrightarrow 2OH_O^{\bullet} \quad (1)$$

The proton produced in anode compartment will permeate the protonic electrolyte membranes in the form of proton defect shown in (1). The electrochemical permeation of H_2 across proton-conductive electrolyte membrane to cathode side reacts with oxygen and produce electricity. The electrochemical extraction of H_2 through proton-conduction membrane in protonic CMFC may act as the membrane catalyzer [9].

One of the major challenges for these perovskite-type proton conductors is a proper compromise between conductivity and chemical stability [10]. Zuo et al. [11] reported a new composition, $Ba(Zr_{0.1}Ce_{0.7})Y_{0.2}O_{3-\delta}$ (BZCY7), exhibited both adequate proton conductivity as well as sufficient chemical and thermal stability over a wide range of conditions relevant to fuel-cell operation. Although the stability of doped $BaCeO_3$ is greatly improved by the introduction of Zr at the B-site, the typical sintering temperature of Zr-replaced $BaCeO_3$ is still above 1550 °C

* Corresponding author. Tel.: +86 551 3606249; fax: +86 551 3607627.
E-mail address: xqliu@ustc.edu.cn (X. Liu).

0378-7753/$ – see front matter © 2008 Elsevier B.V. All rights reserved.
doi:10.1016/j.jpowsour.2008.01.064

[12]. The high sintering temperature has become a major issue for the required low-cost thin-film fabrication technology, and densification sintering is not expected below 1450 °C even for the zirconia-free barium cerates. Several breakthroughs of sintering for these doped $BaCeO_3$ materials have been reported, such as doping transition metal oxides ZnO [12,13]. However, there are still several shortcomings in this method. For example, the introduction of other elements is not appropriate for fabricating a CMFC electrolyte because of thermal expansion mismatch and elemental migration to other cell components. Additionally, due to an evaporation phenomenon of ZnO at 1000 °C during sintering, the accurate amount of ZnO introduced into doped $BaCeO_3$ is quite difficult to determine. Therefore, it is necessary to develop a simple and cost-effective route to fabricate thin protonic electrolyte membranes at a lower temperature in air for the future commercialization of CMFCs.

The simple particle gradation method, which does not need to introduce any other elements, can greatly enhance sintering because it increases the packing density of green electrolyte layer. Besides, some fine powders with high sintering activity in green electrolyte layers will improve sintering [14]. The suspension spray is a low-cost and high efficient method for fabricating inorganic functional ceramic layers [15–17]. The layers could be fabricated in large area and the thickness of electrolyte membranes can also be controlled in expected values. Therefore, suspension spray combined with particle gradation method will be a quite suitable candidate route for preparing dense electrolyte membrane for CMFCs.

In this work, stable $Ba(Zr_{0.1}Ce_{0.7})Y_{0.2}O_{3-\delta}$ (BZCY7) was adopted for the electrolyte materials. The effect of anode composition on anode substrate shrinkage during co-sintering process was studied. The thermal expansion compatibility between sintered anode and electrolyte was subsequently studied under the CMFC operation temperature. A particle gradation method combined with suspension spray was used to fabricate dense electrolyte layers on anode supports. With LSCO cathode, fuel cell was prepared and tested in hydrogen and ammonia and the interface of fuel cell was also investigated.

2. Experimental

2.1. Synthesis of BZCY7 powder

The $Ba(Zr_{0.1}Ce_{0.7})Y_{0.2}O_{3-\delta}$ (BZCY7-1) powders with big average grain size was synthesized by a modified Pechini method [18]. The proper amounts of starting precursors were added into citric acid solution. $Ba(C_2H_3O_2)_2$, $Ce(NO_3)_3{\cdot}6H_2O$, Y_2O_3 and $Zr(NO_3)_4$ were dissolved at the stoichiometric ratio. And the citric acid was then added with citric/metal mole ratio set at 1.2:1, which was used as complexation/polymerization agent. Then this solution was stirred on a heating machine and then changed to brown foam and ignited to flame. The brown ash was subsequently calcined at 1250 °C for 3 h. XRD test was used to detect the phase formation of these fresh powders.

The $Ba(Zr_{0.1}Ce_{0.7})Y_{0.2}O_{3-\delta}$ (BZCY7-2) powders with small average grain size was prepared through a glycine nitrate process [19]. In the process, $Ba(C_2H_3O_2)_2$, $Ce(NO_3)_3{\cdot}6H_2O$, Y_2O_3 and $Zr(NO_3)_4$ at the stoichiometric ratio of BZCY7-2 were dissolved in distilled water. And the glycine acid was then added with glycine/metal mole ratio set at 1:1. Then this solution was stirred on a heating machine and then changed to yellow foam and ignited to flame. The yellow ash was subsequently fired at 1150 °C for 3 h. The particle size distribution of BZCY7-1 and BZCY7-2 powders after ball-milling in ethanol for 24 h was analyzed with a laser particle size analyzer (Jinan PCC-III).

2.2. Preparation of anode

The mixed powders of the fine BZCY7-2 and a commercial Ni_2O_3 powders in different weight ratios (65:35, 50:50, 35:65) were ball-milled for 10 h and then pressed into disks of 15 mm in diameter and 0.65 mm in thickness under 200 MPa. The electrolyte disks (BZCY7-1, BZCY7-2, mixture of BZCY7-1 and BZCY7-2 with 10% BZCY7-2 in weight ratio) were also prepared under the same condition. Then the sintering behaviors of these disks from 30 °C to 1400 °C were detected with a thermal expansion analyzer (PCY-III). Besides, the expansion behaviors from 30 °C to 1000 °C of the disks which were sintered at 1400 °C for 5 h were also detected.

2.3. Preparation of suspensions and electrolytes

With BZCY7-1, BZCY7-2, and mixed powders (with 5% and 10% BZCY7-2 powders in weight ratios), four different suspensions were prepared after ball-milling in ethanol for 24 h. The bulk densities of the four kinds of powders after ball-milling were determined with a home-developed apparatus. With the suspensions, four corresponding green electrolyte layers were deposited on anode supports with the weight ratio of 65:35 between Ni_2O_3 and BZCY7-2. Through a suspension spray method, the electrolyte layers were deposited on anode substrates. After co-sintering at 1400 °C for 5 h, the electrolyte membranes were prepared.

2.4. Preparation and testing of cell

A graded cathode $La_{0.5}Sr_{0.5}Co_{3-\delta}$ was applied onto the electrolyte surface in the area of 0.14 cm^2 and after sintering at 1050 °C for 3 h to assemble a single cell (named as cell-1). The thickness and diameter of fuel cell were 2 mm and 13 mm, respectively. Ag paste was applied onto the cathode surface as the current collector after firing at 550 °C for 30 min. Cell-1 was tested in a home-developed testing system from 650 °C to 700 °C. Hydrogen and ammonia were used as fuel and the static air was used as oxidant. The water vapor concentration in fuel gases was 3% and the flow rate of fuel gases was 40 ml min^{-1}. The interface resistance of cell-1 was tested with an ac impedance (Chenhua 604C, Shanghai). The frequency range is from 10 Hz to 10,000 Hz. The cross-sectional view of cell-1 was observed with a scanning electronic microscope (SEM, JSM-6301F).

Another cell was prepared by a dry-pressing method [20–22] with BZCY7-2 powder and a mixed anode powder in which the weight ratio of Ni_2O_3 65%. After co-sintering at 1400 °C for

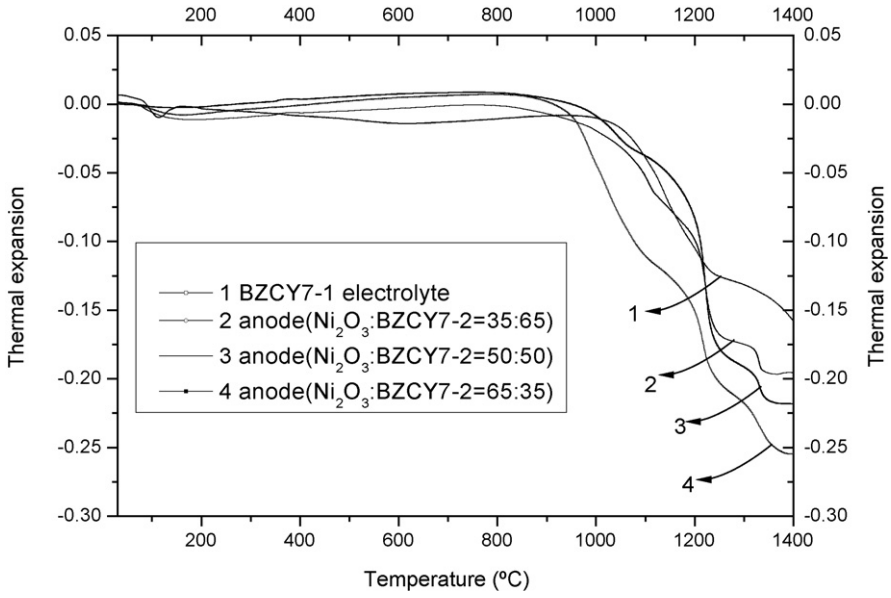

Fig. 1. Shrinkage of green anode and electrolyte during sintering.

5 h and $La_{0.5}Sr_{0.5}CoO_{3-\delta}$ cathode, a fuel cell (named as cell-2) was prepared and tested in ammonia from 650 °C to 700 °C. The interface resistance of cell-2 was tested with ac impedance. The cross-sectional view of cell-2 was observed with a SEM. The gas analysis of ammonia decomposition of two cells was tested with a gas chromatography analyzer (GC102AT) under open circuit conditions.

3. Results and discussion

3.1. Effect of anode composition on anode shrinkage

The XRD test of the as-prepared BZCY7-1 and BZCY7-2 powders indicates a single phase without detection of other impurity phases. Fig. 1 shows the shrinkage behaviors of green anodes and the electrolytes during sintering. It is obvious that there are almost no shrinkages of anodes and electrolytes below 1000 °C. Above 1000 °C, the anodes and electrolytes shrink rapidly because of the changes during sintering. In this process, the adherence of NiO and BZCY7-2 particles to each other forms necks and decreases the pores in anodes and electrolytes, which leads to shrinkages during sintering [23]. However, the shrinkage rates of anodes with different amounts of Ni_2O_3 were all a bit larger than that of electrolytes. This may be because the Ni_2O_3 phase starts to change into NiO phase above 600 °C and the fresh NiO grains grows rapidly during sintering. Meanwhile, the sintering activity of fresh NiO may be also higher than doped $BaCeO_3$ ceramics, which may also result in a big shrinkage of anodes. The shrinkages of anodes increase apparently as the weight content of Ni_2O_3 rises from 35% to 65%. At 1400 °C, the shrinkages of anode with 65% Ni_2O_3 and electrolyte reach as high as 25% and 15%, respectively. As seen in the figure, the electrolyte is not very dense because of the continuous shrinkage trend above 1400 °C. Thus, a big shrinkage margins between anodes and electrolytes will promote the electrolyte densification because of driven sintering from anode substrate shrinkage during co-sintering. For the meanwhile, a high content of Ni_2O_3 in anode can easily form a connected Ni skeleton phase after reducing which was desired for the anode Ni-based skeleton microstructure [24]. Generally, the anode composition was determined as 65% Ni_2O_3 in the weight ratio for substrate of suspension spray.

3.2. Thermal expansion compatibility

Since a good thermal compatibility between anodes and electrolytes of anode-supporting CMFCs is another key point [25]. A thermal expansion mismatch may lead to a bad interface contact between anode and electrolyte, some cracks in electrolyte membrane, even a destruction of cell under operation conditions. Fig. 2 shows the thermal expansion of sintered anode and electrolyte from 200 °C to 1000 °C. The thermal expansion of anode and electrolyte all increases almost at the same rate as the temperature rises. The margins of thermal expansion

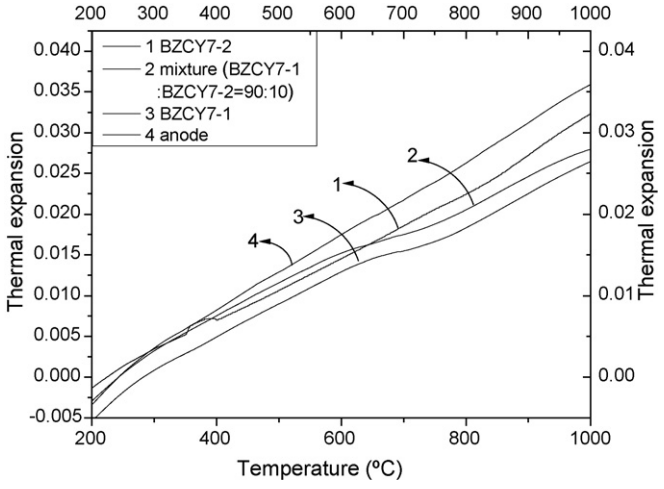

Fig. 2. Thermal expansion of sintered anode and electrolyte.

between anodes and electrolytes are quite small and less than 1% below 750 °C, which indicates a good thermal compatibility at intermediate temperature. From 750 °C to 1000 °C, the margins are very close to 1%, which readily reaches the requirements of thermal expansion compatibility for high-temperature operating conditions. Besides, the electrolytes prepared with three different powders exhibit almost the same thermal expansion behaviors under the same temperature condition, which indicates that the thermal expansion behaviors of electrolytes are irrelevant to the preparation methods of powders. It also proves an advantage that the particle gradation method for electrolyte membranes fabrication does not change the electrolyte thermal expansion behaviors.

3.3. Particle gradation method

The particle size distribution of powders after ball-milling was shown in Fig. 3. It can be seen that the d_{50} of BZCY7-1 and BZCY7-2 powders are 3 μm and 0.8 μm, respectively. When assuming green electrolyte is deposited only with BZCY7-1 powders, then there will be some small pores between big particles in green electrolyte. So the green packing density can be increased by filling the pores with proper amounts of small particles. A higher green density is advantageous for densification during sintering. Besides, some fine powders with high sintering activity in green electrolytes will also improve sintering. Therefore, particle gradation of these two particle sizes could lead to a higher green density and densification. Table 1 shows the bulk densities of four different powders after ball-milling. The bulk densities of two mixtures respectively reach 48.1% and 45.3% while the bulk densities of BZCY7-1 and BZCY7-2 only reach 37.5% and 34.8%, respectively. It is apparent that particle gradation can greatly increases the green packing density.

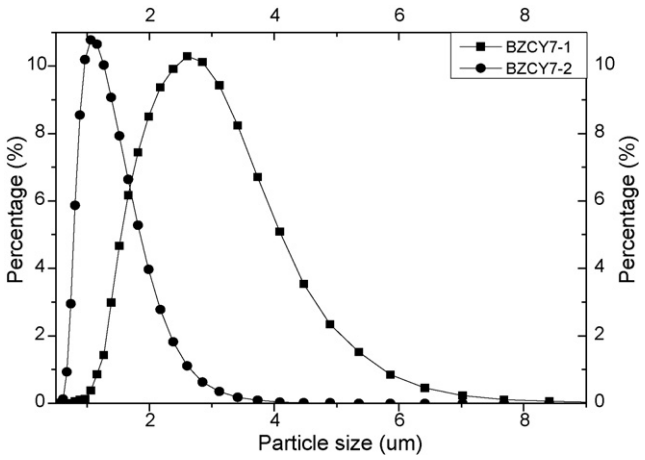

Fig. 3. The particle size distribution of BZCY7-1 and BZCY7-2 powders after ball-milling.

The surface morphologies and the cross-sectional views of electrolytes prepared with four different powders after sin-

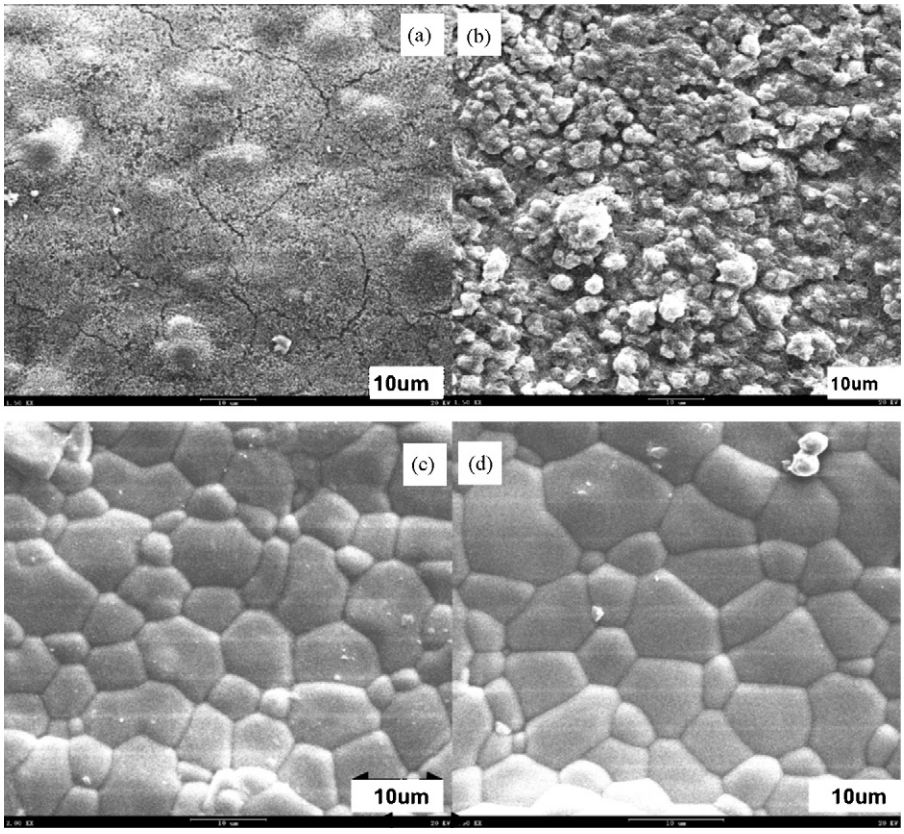

Fig. 4. The surface morphology of electrolyte membranes after sintering. (a) Prepared with BZCY7-2 powders, (b) prepared with BZCY7-1 powders, (c) prepared with BCZY-1 powders mixed with 5% BZCY7-2 powders in weight ratio, and (d) prepared with BZCY7-1 powders mixed with 10% BZCY7-2 powders in weight ratio.

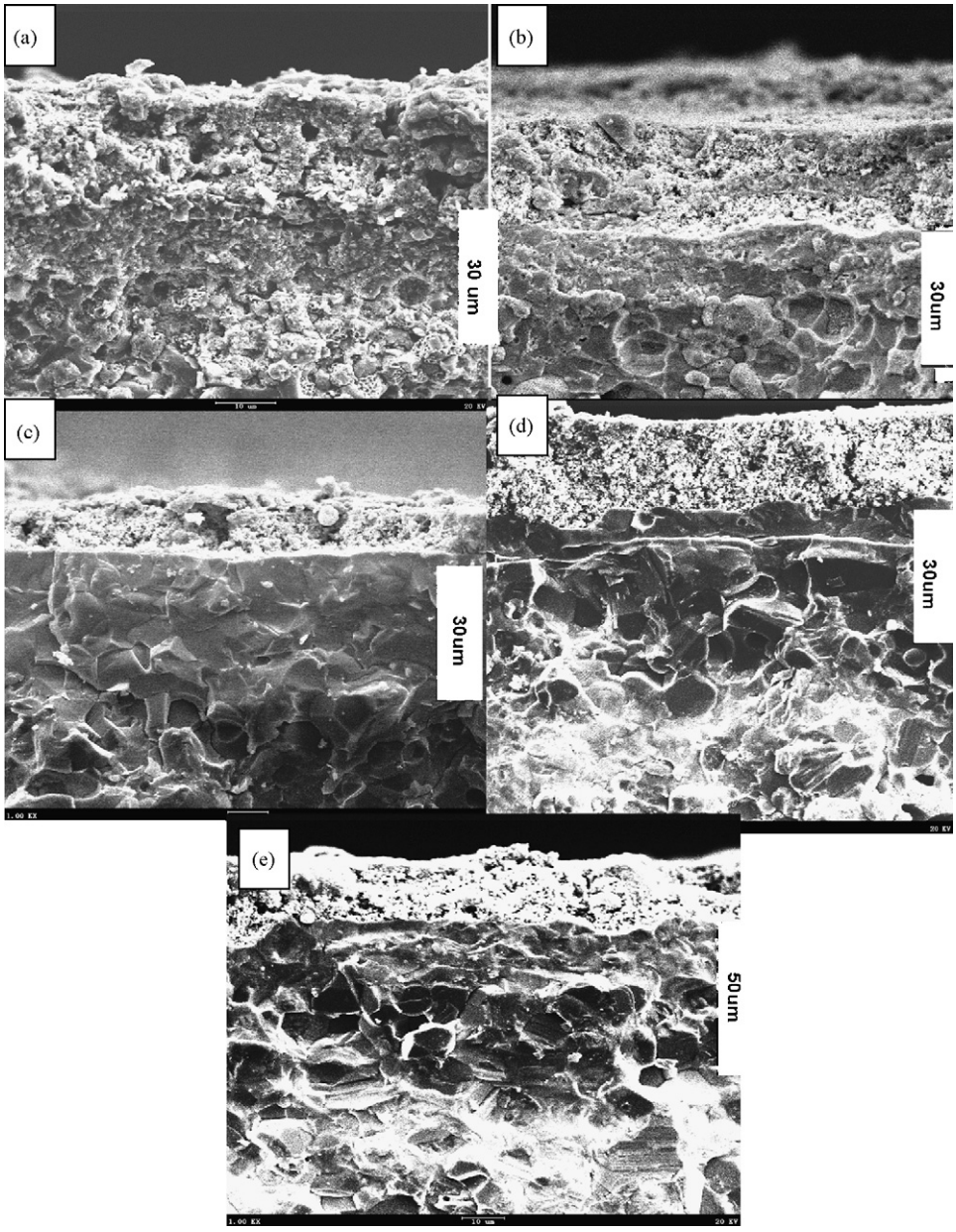

Fig. 5. The cross-sectional view of as prepared electrolytes. (a) Prepared with BZCY7-2, (b) prepared with BZCY7-1, (c) prepared with 5% BZCY7-2 + 95% BZCY7-1 before testing, (d) prepared with 10% BZCY7-2 + 90% BZCY7-1 after testing, and (e) prepared with dry-pressing method with BZCY7-2 after testing.

tering at 1400 °C for 5 h are shown in Figs. 4 and 5. The samples prepared only with BZCY7-1 and BZCY7-2 powder are loose and porous. The surface views of electrolytes prepared with the two different mixtures with BZCY7-2 powders in the weight ratio of 5% and 10% are shown in Fig. 4c and d. As seen in the SEM photos, the electrolyte membranes are very dense and uniform. The big grains and small ones show good adherences, which indicates the particle gradation method could effectively improve the densification during sintering. The grain size in sample d is 4–6 μm which is a bit larger than that of sample c, 3–5 μm. It may be due to the excessively growing of grains in sample d, which has a higher content of fine active BZCY7-2 powders. For the meanwhile, the cross-sectional views of samples prepared with mixtures, which are shown in Fig. 5c and d, also demonstrate that the electrolyte membranes are quite dense after sintering. To sum up, suspension spray combined with particle gradation method for preparing BZCY7 electrolyte membranes is a good route candidate.

Table 1
Bulk densities of four samples

Samples	Bulk density (%)
1	34.8
2	37.5
3	45.3
4	48.1

1, BZCY7-2 powders; 2, BZCY7-1 powders; 3, 95% BZCY7-1 mixed with 5% BZCY7-2 powders in weight ratio; 4, 90% BZCY7-1 mixed with 10% BZCY7-2 powders in weight ratio.

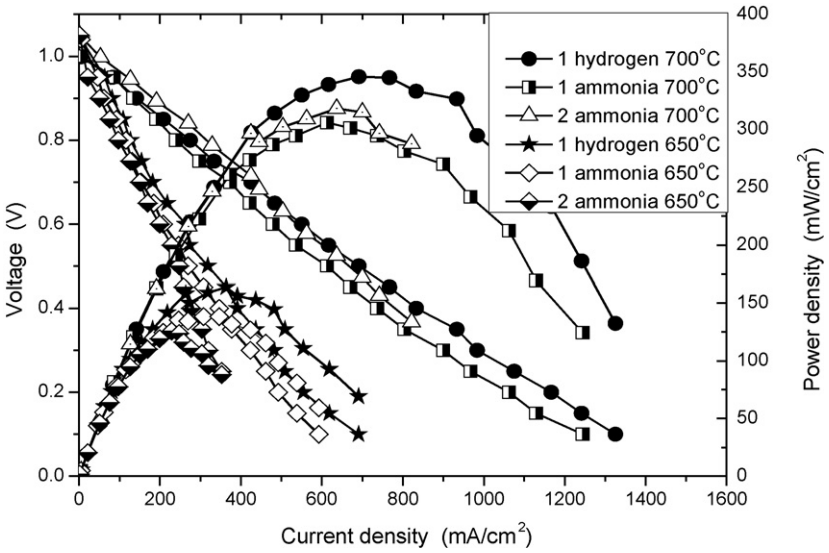

Fig. 6. The performance of cell tested with ammonia and hydrogen.

3.4. Cell performance

The cell performances are showed in Fig. 6. The open circuit voltages (OCVs) of cell-1 and cell-2 are all above 1.0 V at 700 °C and 650 °C in hydrogen and ammonia. They are very close to theoretical values (~1.17 V at 700 °C), which indicates the electrolyte membranes are very dense. The small margins between tested and theoretical OCVs may be due to the electronic conductivity of doped $BaCeO_3$ at high temperature [26]. The outputs of cell-1 are 330 mW cm^{-2} and 300 mW cm^{-2} in hydrogen and ammonia at 700 °C, 140 mW cm^{-2} and 120 mW cm^{-2} in hydrogen and ammonia at 650 °C, respectively. The output of cell-1 at 650 °C in hydrogen is higher than that reported by Hibino et al. [27]. They used a $BaCe_{0.75}Y_{0.25}O_{3-\delta}$ electrolyte with higher conductivity in the thickness of 0.5 mm in a electrolyte-supporting fuel cell. It means that the reduction of electrolyte thickness is an inevitable way to improve cell performance. The peak powder densities of cell-1 in ammonia and hydrogen are quite close to each other at the same temperatures. This demonstrates that ammonia as a fuel candidate is feasible. The small differences of power densities may be due to that the endothermic ammonia cracking reaction decreases the actual operating temperatures.

Table 2 shows the gases analysis of ammonia fuel decomposition in cell-1 at 700 °C and 650 °C. The hydrogen partial pressures in cell-1 fueled with ammonia are only about 74% of the total pressure. The ammonia almost completely decomposes above 650 °C. Meanwhile, the NO-free mixed gases also indicate an advantage of using ammonia fuel for protonic CMFCs. While the cell-1 fueled with hydrogen has the high hydrogen partial pressure values of about 97% of the total pressure.

Table 2
Gases analysis of ammonia decomposition under open circuit condition

Temperature (°C)	Gas			
	H_2	N_2	NH_3	H_2O
700	74.0%	24.5%	0.1%	1.4%
650	73.8%	24.7%	0.1%	1.4%

Though the different hydrogen contents in the two fuels, the hydrogen partial pressures or the proton concentrations on the electrolyte surface in anode compartment may be very close to each other as the hydrogen or proton diffuses faster toward the interface than N_2 does. This may be another reason which leads to small differences of peak power densities in two fuels. Comparatively, cell-2 at 700 °C exhibits a performance of 305 mW cm^{-2} in ammonia. This is very close to that of cell-1 even the electrolyte thickness of cell-2 is 50 μm. As seen from Fig. 5d, the anode of cell-1 may be not completely reduced into BZCY7 + Ni, which may increase the total resistance and reduce the outputs. Assuming the electrolyte thickness of cell-1 is 30 μm, the electrolyte conductivity of cell-1 may also prove this point though calculating the BZCY7 electrolyte conductivities from ac impedance spectra shown in Fig. 7. The calculated conductivity of electrolyte in cell-1, 0.008 S cm^{-1}, is a little smaller than that of cell-2, 0.01 S cm^{-1} at 700 °C, while the reported values are 0.012 S cm^{-1} at 700 °C and 0.01 S cm^{-1} at 650 °C, respectively [11]. The small differences between calculated conductivities and reported values may be due to different preparation methods of electrolyte materials. At 650 °C, the two cells exhibited similar phenomenon compared with that at 700 °C. In general, the electrolyte membrane fabricated with this combined technique exhibited comparable performances as that prepared by the classical-laboratory dry-pressing method, which indicated that this technique is a potentially promising route for preparation of protonic ceramic electrolyte membranes.

3.5. Interface of cell

The interface resistances of cell-1 and cell-2 at 700 °C are shown in Fig. 7. It is obvious that the interface resistances of

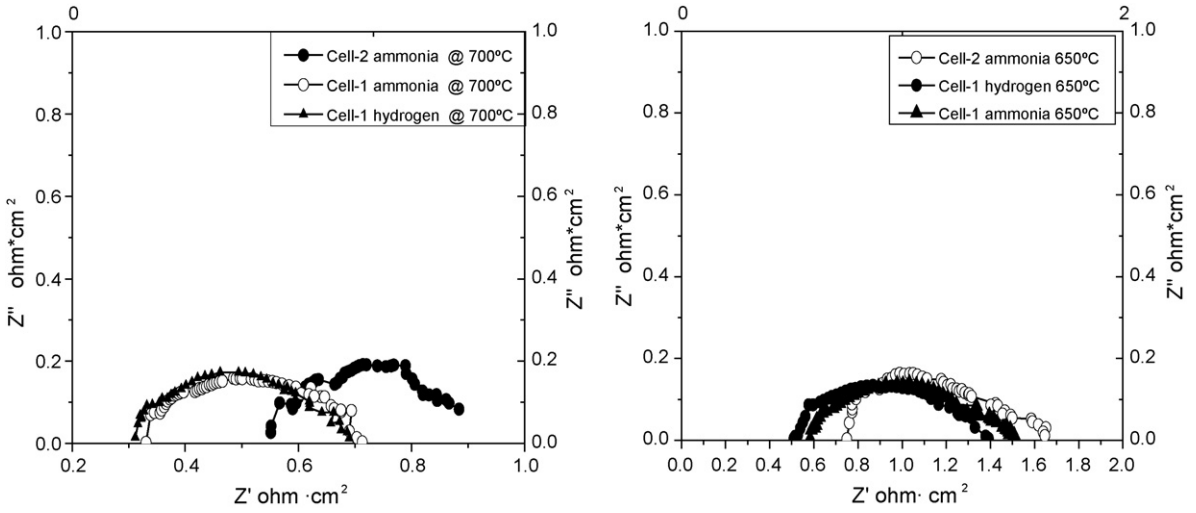

Fig. 7. The resistance of cell-1 and cell-2 tested with ac impedance at 650 °C and 700 °C.

Table 3
Interface resistances of cell-1 and cell-2

Fuel and temperature	Interface resistance	
	Cell-1 ($\Omega\,cm^2$)	Cell-2 ($\Omega\,cm^2$)
Ammonia@700 °C	0.38	0.35
Ammonia@650 °C	0.82	0.80

cell-1 and cell-2 in ammonia have the similar values, about $0.38\,\Omega\,cm^2$ at 700 °C and about $0.82\,\Omega\,cm^2$ at 650 °C, seen from Table 3, respectively. This means the interface resistances of cell-1 prepared with this combined technique is as good as that of cell-2 prepared with classical dry-pressing method. Additionally, the interface resistances of the two cells increases rapidly as the temperature drops from 700 °C to 650 °C, which may be due to the decline of catalytic activity and the drop of conductivities of electrodes. The interface resistances of cell-1 exhibit smaller values in hydrogen than that in ammonia at corresponding temperatures, which may be because the endothermic cracking reaction of ammonia decreases the actual operating temperature. Generally, the interface of cell-1 prepared with this combined technique is comparable to that of cell-2 prepared with dry-pressing method.

4. Conclusion

BZCY7-1 and BZCY7-2 powders with two different particle sizes (d_{50}), 3 μm and 0.8 μm, respectively, are synthesized through Pechini method and glycine nitrate process. A proper anode composition with 65% Ni_2O_3 in weight ratio is determined for preparing anode substrates. Meanwhile, the margins of thermal expansion between the sintered electrolyte and anode are smaller than 1% from 30 °C to 750 °C. By a suspension spray combined with particle gradation method, in which the weight ratio range of BZCY7-2 is from 5% to 10%, dense electrolyte membranes are successfully prepared on the anode substrates. The cell prepared with the combined technique exhibits higher outputs, which are $330\,mW\,cm^{-2}$ in hydrogen and $300\,mW\,cm^{-2}$ in ammonia at 700 °C, respectively. The interface resistance of this cell exhibits a comparable value, $0.38\,\Omega\,cm^2$ at 700 °C, to that of a cell prepared by classical dry-pressing method. To sum up, this combined technique can be considered as commercial fabrication technology candidate. Therefore, the suspension spray process combined with particle gradation method for preparation of ceramic electrolyte membranes is a suitable candidate technique for the future commercialization of solid oxide fuel cells.

Acknowledgements

The authors would like to thank the financial support from Chinese Natural Science Foundation on contract No. 50572099 and 50730002 and Chinese Research Foundation for the Doctors (20060358034).

References

[1] G. Meng, G. Ma, Q. Ma, R. Peng, X. Liu, Solid State Ionics 178 (2007) 697.
[2] A.K. Demin, P.E. Tsiakaras, V.A. Sobyyanin, S.Yu. Hramova, Solid State Ionics 152–153 (2002) 555.
[3] H. Iwahara, T. Esaka, H. Uchida, Solid State Ionics 3–4 (1981) 359.
[4] H. Iwahara, H. Uchida, J. Electrochem. Soc. 135 (1988) 529.
[5] D.J.D. Corcorana, D.P. Tunstallb, J.T.S. Irvine, Solid State Ionics 136–137 (2000) 297.
[6] N. Zakowsky, S. Williamson, J.T.S. Irvine, Solid State Ionics 176 (2005) 3019.
[7] C. Zuo, M. Liu, J. Am. Chem. Soc. 231 (2006) 521.
[8] A.K. Azad, J.T.S. Irvine, Solid State Ionics 178 (2007) 635–640.
[9] S. Hamakawa, T. Hibino, H. Iwahara, J. Electrochem. Soc. 459 (1993) 140.
[10] M.J. Scholten, J. Schoonman, J.C. Vanmiltenburh, H. Oonk, Solid State Ionics 83 (1999) 61.
[11] C. Zuo, S. Zha, M. Liu, M. Hatano, M. Uchiyama, Adv. Mater. 18 (2005) 3318.
[12] S. Tao, J.T.S. Irvine, Adv. Mater. 18 (2006) 1581.
[13] P. Babilo, S.M. Haile, J. Am. Ceram. Soc. 88 (2005) 2362.
[14] W. Bao, W. Zhu, G. Zhu, J. Gao, G. Meng, Solid State Ionics 176 (2005) 669.
[15] K. Xie, Q. Ma, B. Lin, X. Liu, G. Meng, J. Power Sources 170 (2007) 38.

[16] R. Yan, D. Ding, B. Lin, M. Liu, G. Meng, X. Liu, J. Power Sources 164 (2007) 567.
[17] B. Lin, W. Sun, K. Xie, Y. Dong, D. Dong, X. Liu, J. Gao, G. Meng, J, Alloys Compd., 2007, doi:10.1016/j.jallcom.2007.10.063.
[18] G.X. Wang, D.H. Bradhurst, H.K. Liu, S.X. Dou, Solid State Ionics 120 (1999) 95.
[19] R. Peng, W. Yan, Y. Lihai, M. Zongqiang, Solid State Ionics 177 (2006) 389–393.
[20] C. Xia, M. Liu, J. Am. Ceram. Soc. 84 (2001) 1903.
[21] X. Changrong, L. Meilin, Solid State Ionics 144 (2001) 249.
[22] M. Qianli, P. Ranran, L. Yongjing, G. Jianfeng, M. Guangyao, J. Power Sources 161 (2006) 95.
[23] R. Yan, F. Chu, Q. Ma, X. Liu, G. Meng, Mater. Lett. 60 (2006) 3605.
[24] S. Ohara, R. Maric, X. Zhang, K. Mukai, T. Fukui, H. Yoshidab, T. Inagaki, K. Miura, J. Power Sources 86 (2000) 455.
[25] E. Ivers-Tiffé, A. Weber, D. Herbstritt, J. Eur. Ceram. Soc. 21 (2001) 1805.
[26] N. Tanigushi, K. Hatoh, J. Niikura, T. Gamo, Solid State Ionics 53–56 (1992) 998.
[27] T. Hibino, A. Hashimoto, M. Suzuki, M. Sano, J. Electrochem. Soc. A1503–A1508 (2002) 149.